ALISA

Noble, Anna; Guille, Matthew; Cobley, James N

Published in:
Free Radical Biology & Medicine
Publication date:
2021

Free Radical Biology and Medicine xxx (xxxx) 1–10

Contents lists available at ScienceDirect

Free Radical Biology and Medicine

journal homepage: www.elsevier.com/locate/freeradbiomed

Original research

ALISA: A microplate assay to measure protein thiol redox state

Anna Noble [a], Matthew Guille [a], James N. Cobley [b,*]

[a] European Xenopus Resource Centre, Portsmouth University, Portsmouth, PO1 2DY, UK
[b] Redox Biology Group, UHI, Inverness, IV2 3JH, UK

ARTICLE INFO

Keywords:
Protein thiol
Oxidative stress
Reactive oxygen species
Development
Redox signalling

ABSTRACT

Measuring protein thiol redox state is central to understanding redox signalling in health and disease. The lack of a microplate assay to measure target specific protein thiol redox state rate-limits progress on accessibility grounds: redox proteomics is inaccessible to most. Developing a microplate assay is important for accelerating discovery by widening access to protein thiol redox biology. Beyond accessibility, enabling high throughput time- and cost-efficient microplate analysis is important. To meet the pressing need for a microplate assay to measure protein thiol redox state, we present the **A**ntibody-**L**inked **O**x**i**-**S**tate **A**ssay (ALISA). ALISA uses a covalently bound capture antibody to bind a thiol-reactive fluorescent conjugated maleimide (F-MAL) decorated target. The capture antibody-target complex is labelled with an amine-reactive fluorescent *N*-hydroxysuccinimide ester (F–NHS) to report total protein. The covalent bonds that immobilise the capture antibody to the epoxy group functionalised microplate enable one to selectively elute the target. Target specific redox state is ratiometrically calculated as: F-MAL (i.e., reversible thiol oxidation)/F–NHS (i.e., total protein). After validating the assay principle (i.e., increased target specific reversible thiol oxidation increases the ratio), we used ALISA to determine whether fertilisation—a fundamental biological process—changes Akt, a serine/threonine protein kinase, specific reversible thiol oxidation. Fertilisation significantly decreases Akt specific reversible thiol oxidation in *Xenopus laevis* 2-cell zygotes compared to unfertilised eggs. ALISA is an accessible microplate assay to advance knowledge of protein thiol redox biology in health and disease.

1. Introduction

The chemical biology of oxygen derived free radical (e.g., superoxide) and non-radical (e.g., hydrogen peroxide) molecules termed Reactive Oxygen Species (ROS) gives rise to positive (e.g., redox signalling) and negative (e.g., oxidative damage) functionality in health and disease [1–3]. Understanding their pleiotropic biology relies on measurement techniques [4,5]. Disregarding overtly flawed assays (e.g., thiobarbituric acid-reactive substances assay, TBARS) [6], the ability to measure ROS [7], antioxidant enzyme activity and/or content [8], oxidised macromolecule adducts [3], and major cellular outcomes (i.e., cell adaptation, injury, and death) using a plate reader or other readily accessible technique (i.e., immunoblotting [9]) helped unravel their negative functionality. As Halliwell and Whiteman review [10], plate reader compatible oxidised macromolecule assays amongst other techniques implicated ROS in diseases betokening a role for oxidative stress as originally formulated by Sies (i.e., antioxidant-pro-oxidant imbalance induced oxidative damage) [11]. Sies and colleagues have redefined oxidative stress to include pathologically disrupted redox signalling and coined oxidative eustress to define physiological redox signalling [12–16]. Unlike the formidable analytical arsenal available to assess oxidative damage in a plate reader, the field lacks a microplate assay to assess redox signalling by measuring target specific protein thiol redox state.

Sulphur chemistry endows protein thiols with the ability to play diverse catalytic, antioxidant, structural, and allosteric roles and orchestrate redox signalling symphonies via their one and two electron ROS reactivity [17–21]. One and two electron ROS reactivity can be direct (i.e., biomolecular reaction between a specific ROS and the target thiol) and indirect (i.e., electron exchange via intermediates [22–25]). As Held remarks [26], protein thiols can sense, amplify, toggle, oscillate, and suppress redox signals. Reversible thiol oxidation can transmit a redox signal by changing protein activity, locale, interactome, phase, and lifetime [27–29]. The thioredoxin and glutathione dependent redox machinery bidirectionally controls protein thiol redox state by adding or subtracting electrons to impart specificity and reversibility [21]. The foundational importance of redox signalling makes it essential to be able to measure target specific protein thiol redox state. The lack of an

* Corresponding author.
E-mail address: james.cobley@uhi.ac.uk (J.N. Cobley).

https://doi.org/10.1016/j.freeradbiomed.2021.08.018
Received 12 July 2021; Received in revised form 11 August 2021; Accepted 17 August 2021
0891-5849/

accessible plate reader assay allied to the caveats of immunological techniques means target specific protein thiol redox state is usually assessed using redox proteomic workflows [30–32]. Developing a microplate to measure target specific protein thiol redox state is important because:

1. It would create a new, redox proteomic complementary, methodological pillar to determine whether an experimental stimulus or state changes target specific protein thiol redox state.
2. Lack of an analogue to the formidable cannon of microplate compatible techniques to measure ROS, antioxidant enzyme activity and/or content, oxidised macromolecule adducts, and major cellular outcomes rate-limits progress on accessibility grounds. Current knowledge of oxidative stress would markedly decrease if the microplate compatible assays used in decades of research were inaccessible. In reverse, a microplate assay to measure target specific protein thiol redox state could accelerate discovery by widening access to the field.
3. Unlike methodologically flawed assays (e.g., TBARS [6]), a microplate assay to measure target protein thiol redox state would stand on valid analytical ground. Redox proteomic sample processing procedures using chemically defined labelling reagents and workflows can be repurposed to support a microplate assay. The reporters used to validly assess protein thiol redox state in a mass spectrometer can, when substituted for a compatible reporter (i.e., a mass change is of limited value), be used in a microplate assay. Technical updates, that, for example, afford sulfenic acid orthogonality when labelling reduced thiols or direct chemotype reactivity (e.g., direct disulfide bond labelling), can be installed as the chemical toolkit evolves [33].
4. Reporting the target specific thiol redox state as the sum of all labelled thiols, is inherently valuable. To illustrate the point, consider the value of measuring ROS using various reporters from exo-markers [34], genetically-encoded redox sensors [35], and small molecule fluorophores [36]. The underlying chemistry means that most reporters measure the “global” level of a subset of ROS (e.g., boronate probes react with hydrogen peroxide and peroxynitrite [7]). Their ability to do so is invaluable. For example, exo-markers helped unravel how ageing perturbs mitochondrial ROS production [34]. By analogy reporting global target specific thiol redox state (i.e., the signal is the sum of the aggregated mean of all modifiable cysteine residues on the target) is important. Unlike ROS reporters, the result is a true global measure (i.e., exogenous ROS reporters are in competition with endogenous antioxidant enzymes) that reports what ROS do (i.e., redox functionality). That many targets are incompletely (i.e., some cysteine residues are unreported) and some are undetected (i.e., hydrophobic, low abundant, and/or difficult to digest/ionise/fragment targets) by redox proteomics adds value. A microplate could be useful for confirming the observed redox proteomic change; particularly if any false discovery doubts were immunologically eliminated.
5. Plate reader assays possess several important advantages including automated high-throughput analysis, as well as, cost- and time-efficiency. For example, cost- and time-efficient plate reader analysis could enable one to rapidly screen several proteins and thereby select "hits" for follow-up redox proteomic and/or functional analysis.

To meet the pressing need for a microplate assay to measure target protein thiol redox state, we present the **A**ntibody-**L**inked Ox**i**-**S**tate **A**ssay (ALISA). ALISA uses a capture antibody to bind a fluorescent thiol redox state reporter decorated target and a total protein reporter to ratiometrically quantify target protein thiol redox as reversible thiol oxidation (i.e., the fluorescent thiol redox state reporter signal) relative to total protein. After validating the assay principle (i.e., increased target reversible thiol oxidation increases the ratio), we show that: ALISA can quantify target reversible thiol oxidation in a plate reader and a fundamental biological process alters the redox state of a strategically important target. Specifically, fertilisation decreases Akt—a serine/threonine protein kinase—specific reversible thiol oxidation in *Xenopus laevis* (*X. laevis*). This proof-of-principle finding demonstrates that ALISA can measure target specific protein thiol redox state in a microplate.

2. Results

2.1. ALISA: A microplate assay to measure protein thiol redox state

The **A**ntibody-**L**inked Ox**i**-**S**tate **A**ssay (ALISA) comprises a: (1) capture antibody; (2) thiol redox state reporter; and (3) total protein reporter. An immobilised capture antibody is used to bind a fluorescent maleimide (F-MAL) labelled target and an amine-reactive *N*-hydroxysuccinimide ester functionalised fluorophore (F–NHS) is used to internally normalise the F-MAL signal (Fig. 1). Specifically, the capture antibody is covalently bound to an epoxy group functionalised mi-

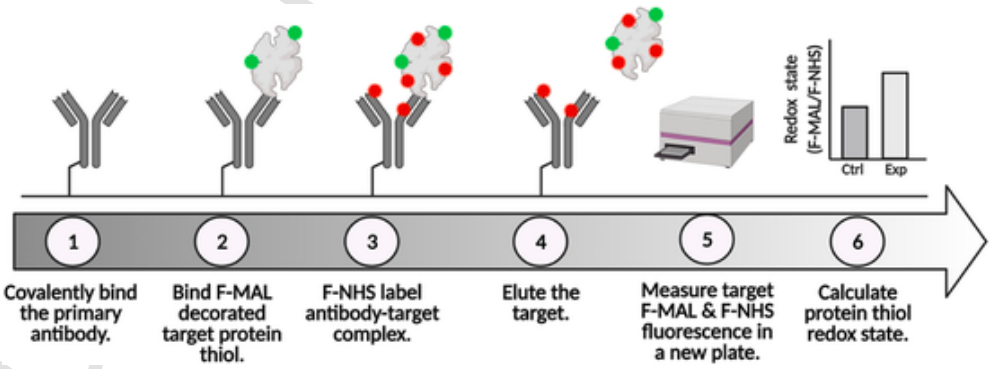

Fig. 1. ALISA: A microplate assay to measure protein thiol redox state. 1. A capture antibody is covalently bound to an epoxy group functionalised plate via biomolecular nucleophilic substitution chemistry. Blocking and wash steps are omitted for clarity. 2. The immobilised capture antibody is used to bind a fluorescent maleimide (F-MAL, green dots) decorated target protein from a biological sample (e.g., cell lysate). 3. After washing away contaminants (omitted for clarity), the capture antibody-target complex is labelled with an amine-reactive fluorescent *N*-hydroxysuccinimide ester (F–NHS, red dots). 4. After removing excess F–NHS by washing (omitted for clarity), the target is selectively eluted (i.e., the covalent bonds prevent the capture antibody from co-eluting with the target). 5. After transferring the eluted target to a new microplate, target specific F-MAL and F–NHS fluorescence is measured in a plate reader. 6. Target specific protein thiol redox state is ratiometrically calculated as: F-MAL (i.e., reversible thiol oxidation)/F–NHS (i.e., total protein). (For interpretation of the references to colour in this figure legend, the reader is referred to the Web version of this article.)

croplate via nucleophilic substitution chemistry. Optionally, a different covalent chemistry can be used to immobilise the capture antibody. To assess reversible thiol oxidation: (1) reduced thiols are alkylated with *N*-ethylmaleimide (NEM) or equivalent; (2) reversibly oxidised thiols are reduced using 1-4-dithiotheitol (DTT) or equivalent; and (3) labelled with F-MAL (e.g., Flouorescin-5-maleimide) or equivalent (note the thiol reactive handle should be the same as step 1—no mixing of maleimide and iodoacetamide, for example, owing to labelling nuances [37]). Optionally, one can selectively quantify a reversibly oxidised chemotype of interest using selective reductants or direct reactivity strategies (i.e., glutaredoxin system to reduce mixed disulfides) [38,39]. To assess reduced thiols, steps 2 and 3 are omitted and NEM is replaced with F-MAL in step 1. To bind the F-MAL decorated target, samples are incubated with the capture antibody functionalised microplate. To internally normalise F-MAL to total protein, the washed capture antibody-target complex is labelled with F–NHS (e.g., AlexaFluor™647 NHS). The covalent bonds between the capture antibody and the epoxy group functionalised microplate enables one to selectively elute the target by disrupting the non-covalent ionic, hydrophobic, hydrogen, and van der Waals chemistry responsible for epitope-paratope binding. After transferring the eluent to a new microplate, target specific redox state is calculated as: F-MAL (i.e., reversibly oxidised thiols)/F–NHS (i.e., total protein). If a matched antibody pair or commercial ELISA is available, one can omit F–NHS and normalise F-MAL to total protein using a biotin-conjugated detector antibody and recombinant protein standard curve; which we term ELISA-ALISA. The assay principle is that: a change in reversible thiol oxidation will change the ratio (i.e., increased reversible thiol oxidation will increase the ratio).

2.2. Covalent bonds immobilise the capture antibody to the epoxy group decorated microplate

If no matched pair antibody or commercial ELISA is available, ALISA requires a covalent bond between the capture antibody and the epoxy functionalised microplate to deconvolute the capture antibody-target F–NHS signal. In F–NHS mode, it is, therefore, essential to demonstrate capture antibody binding capacity and covalent bonding (i.e., the inability of the capture antibody to co-elute with a target). Capture antibody binding capacity is evidenced by the fluorescence emanating from epoxy plate immobilised F–NHS labelled isotype rabbit immunoglobin (IG) compared to unlabelled controls (Fig. 2A). Covalent bonding is evidenced by the IG F–NHS wells retaining their fluorescence after being incubated in denaturing buffer (Fig. 2B). Covalent bonding is further confirmed by immunoblot as a lack of a secondary antibody positive bands in the epoxy plate eluent compared to the positive control (Fig. 2C). The ability of epoxy groups to form covalent bonds with the capture antibody makes F–NHS mode ALISA possible.

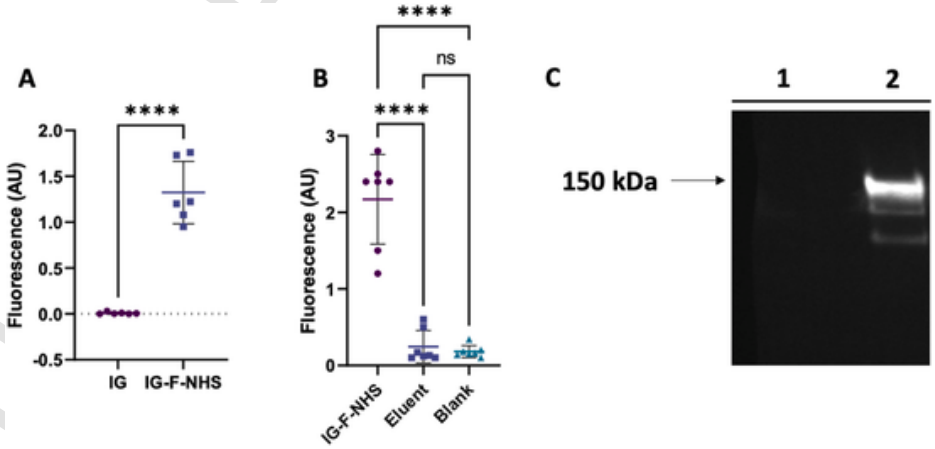

Fig. 2. Covalent bonds immobilise the capture antibody to the epoxy group decorated microplate. A. Fluorescence of an F–NHS rabbit immunoglobulin (IG-F-NHS, $n = 6$) compared to untreated controls (IG, $n = 6$). Significance ($P = <0.0001$) is derived from an unpaired two-tailed Student's t-test. B. IG F–NHS (IG-F-NHS, $n = 7$) epoxy well fluorescence compared to the eluted (i.e., fluorescence of sample buffer incubated with the IG-F-NHS wells) and blank wells. *P* values are derived from a one-way ANOVA with post-hoc Tuckey multiple comparisons testing. IG-F-NHS wells significantly differ from the eluent ($P = <0.0001$) and blank ($P = \leq 0.0001$). There is no statistical difference ($P = 0.9411$) between the eluent and blank wells. C. Immunoblot image of eluents from the IG-F-NHS well eluents (lane 1) compared to the IG control (lane 2) probed with a secondary antibody to detect rabbit IG.

2.3. ALISA can measure Akt specific reversible thiol oxidation in a microplate

To validate ALISA, we selected the serine/threonine protein kinase Akt because it is a strategically important translationally relevant redox regulated target [40,41]. For example, intramolecular disulfide bonds between distinct thiols can activate and inhibit Akt activity [40,41]. To unravel whether a fundamental biological process (i.e., fertilisation) changes Akt redox state, we used *X. laevis*—a tractable developmental model [42]—to validate ALISA. Akt sequence and cysteine residues are highly conserved in *X. laevis* (supplementary Table 1). We engineered 20 or 40% reversibly oxidised redox states by mixing completely F-MAL (i.e., positive) or NEM (i.e., negative) labelled *X. laevis* lysates as appropriate (see methods). We selected the 20% redox state because many cysteines exhibit a basal oxidation level of 20%; which is close to the global thiol proteome level (i.e., 10–15%) [27,43]. Meanwhile, we selected 40% to mimic a response to a redox stimulus and because some cysteines exhibit 40% oxidation at baseline (i.e., the selected states buttress the basal range and simultaneously mimic a response to a redox stimulus).

Akt capture antibody functionalised microplates were incubated with 20 or 40% reversibly oxidised redox states, as well as, 0 (i.e., NEM only) and 100% (i.e., completely F-MAL labelled) reversibly oxidised controls. Consistent with capture antibody dependency (i.e., specificity), no F-MAL signals were observed in isotype IG control wells treated with 100% F-MAL labelled controls (Fig. 3A). Note, it is vital to check for oxidative stress induced non-specific binding (e.g., a diamide treated control) and/or decreased capture antibody binding (e.g., check F–NHS or biotin-conjugated detector antibody signal) when operating ALISA in reduced thiol mode. That is, labelling reduced thiols with F-MAL to detect an increase in reversible thiol oxidation as decreased F-MAL fluorescence relative to total protein. While no F-MAL signal was observed in the 0% group, Akt specific F-MAL signals were observed in the 100, 40, and 20% reversibly oxidised groups (Fig. 3B). Consistent with the ability to discern between different redox states, F-MAL fluorescence was substantially increased in the 40 compared to 20% reversible oxidised group. This could, however, reflect differential target capture (i.e., more Akt captured in the 40% state); which limits it to qualitative analysis due the lack of an internal control. Together F–NHS and covalent bonds transform ALISA into a quantitative assay by affording an internal control and a means to selectively elute the target, respectively. The lack of an F-MAL signal, which can only emanate from the target, in the epoxy plate after elution evidences successful Akt release (Fig. 3C). ALISA reveals a significant difference between the 20 and 40% reversibly oxidised thiol redox states (Fig. 3D). A biotin-conjugated Akt detector antibody coupled to streptavidin conjugated horseradish peroxidase (HRP) mediated colorimetric analysis verifies the ability of ALISA to detect Akt (i.e., specificity, Fig. 3E). Moreover, a recombinant Akt standard curve showcases picogram sensitivity (Fig. 3F). Given accessible immunological techniques to measure protein thiol redox state are available [44], we compared the efficacy of ALISA to a representative immunological technique. Specifically, Click-PEG wherein clickable poly-ethylene glycol (PEG) payloads make reversibly oxidised thiols detectable as mass shifted bands by immunoblot [45–48]. Click-PEG failed to report Akt redox state because the PEG-conjugates were undetectable likely owing to sterically impaired primary antibody binding (Fig. 3G). Provided a suitable capture antibody is available, the evident antibody compatibly of a small molecule F-MAL reporter means most targets should be compatible with ALISA. ALISA achieves an important technical feat: the ability to measure Akt specific thiol redox state in a microplate.

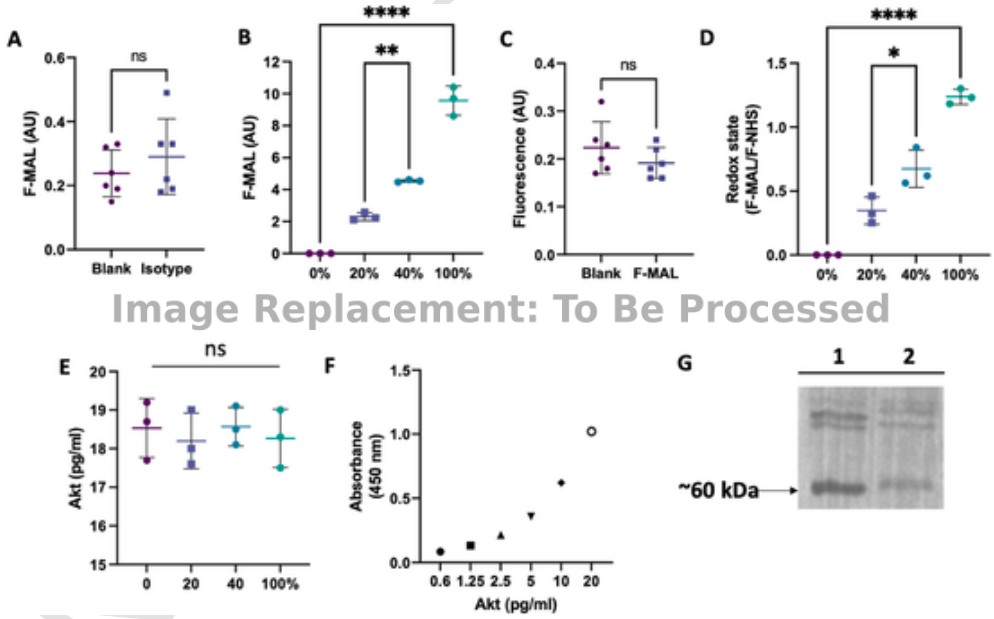

Fig. 3. ALISA can measure Akt specific reversible thiol oxidation in a microplate. No significant (unpaired *t*-test, $P = 0.3846$) difference in F-MAL fluorescence of blank ($n = 6$) compared to isotype control wells ($n = 6$). B. A significant ($P = 0.0018$) difference, as determined by a one-way ANOVA with post-hoc Tuckey multiple comparisons testing, in Akt specific F-MAL fluorescence of 20% ($n = 3$) compared to 40% ($n = 3$) reversibly oxidised standards. The 0 ($n = 3$) and 100% ($n = 3$) reversibly oxidised standards also significantly differed($P < 0.0001$). Other between group statistical comparisons (e.g., 0 vs 20%) are omitted for clarity. C. No significant (unpaired *t*-test, $P = 0.2505$) difference in F-MAL fluorescence in blank ($n = 6$) compared to F-MAL eluted wells ($n = 6$). D. A significant ($P = 0.0125$), as determined by a one-way ANOVA with post-hoc Tuckey multiple comparisons testing, difference in Akt specific reversible thiol oxidation in 20 ($n = 3$) compared to 40% ($n = 3$) reversibly oxidised standards. The 0 ($n = 3$) and 100% ($n = 3$) reversibly oxidised standards also significantly differed ($P = < 0.0001$). Other between group statistical comparisons (e.g., 0 vs 20%) are omitted for clarity. E. Successful detection of Akt using the epoxy functionalised microplate combined with reagents from a commercially available ELISA kit. No significant ($P = 0.8835$), as determined by a one-way ANOVA, between group difference in Akt content. F. Picogram detection of recombinant human Akt using the epoxy group functionalised plate derivatised with an Akt capture antibody. G. An *anti*-Akt Click-PEG immunoblot in *X. laevis* lysates. Note the absence of an azide PEG induced mobility shift (lane 2) compared to the dibenzocyclooctyne PEG4 maleimide only control (lane 1). The uncropped image for panel 3G is presented in supplementary Fig. 1.

2.4. Fertilisation increases Akt specific reversible thiol oxidation

After validating the assay, we used ALISA to determine whether fertilisation alters Akt redox state. To do so, we measured Akt specific reversible thiol oxidation in unfertilised *X. laevis* eggs and 2-cell zygotes (i.e., 90 min post-fertilisation). Akt is a contextually relevant target because fertilisation primes Akt activity by increasing threonine 308 phosphorylation [49]. Consistent with decreased Akt specific F-MAL fluorescence (Fig. 4A), ALISA reveals a significant fertilisation induced decrease in Akt specific reversible thiol oxidation in 2-cell zygotes compared to unfertilised eggs (Fig. 4B). Specificity is further evidenced by the lack of F-MAL signal in isotype IG control wells and positive biotin-conjugated detector antibody signal in eggs and zygotes compared to IG control wells (Fig. 4E–F). That is, no Akt is detected when a fully labelled F-MAL sample is incubated with the isotype control. To exclude any potential F–NHS artefact (i.e., differential hydrolysis and/or structural or post-translational lysine masking), we generated new samples and measured reversible thiol oxidation relative to total Akt (i.e., ELISA-ALISA). ELISA-ALISA confirmed the significant fertilisation induced decrease in Akt specific reversible thiol oxidation in 2-cell zygotes compared to unfertilised eggs (Fig. 4C–D). Unfortunately, we were unable to assess the impact of reducing reversibly oxidised Akt in unfertilised eggs or even compare Akt activity between the two states because quenching the DTT present in commercial kinase buffer with equimolar NEM or removing it with a spin column significantly decreased recombinant human Akt activity (Fig. 4G). The fertilisation induced decrease in Akt specific reversible thiol oxidation demonstrates how ALISA can be used to determine whether an experimental redox stimulus or state changes target specific protein thiol redox state.

2.5. No impact of fertilisation on Src specific thiol redox state

To test whether a small molecule F-MAL reporter makes it possible to assess a selected target provided a suitable capture antibody is available, we measured the redox state of the tyrosine protein kinase Src. Importantly, reversible thiol oxidation regulates Src activity [50], fertilisation activates Src in *X. laevis* [51], and Src led us to develop macroscale ALISA. By measuring Src, we could also evaluate whether

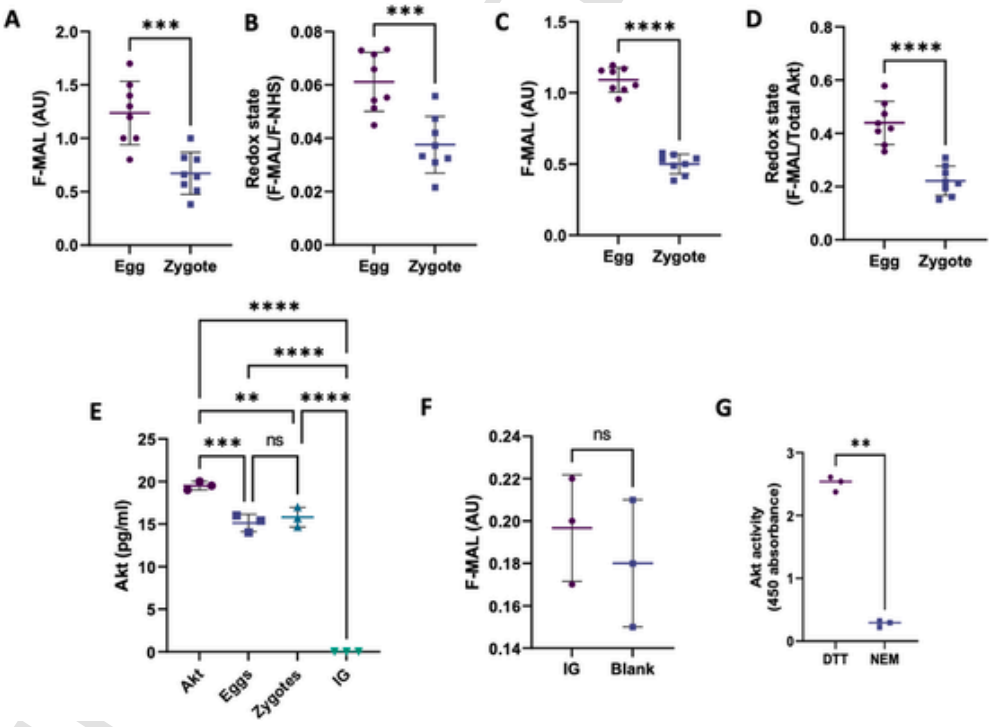

Fig. 4. Fertilisation increases Akt specific reversible thiol oxidation. A. A significant ($P = 0.0005$) fertilisation induced decrease in Akt F-MAL fluorescence in 2-cell zygotes compared to unfertilised eggs. B. A significant ($P = 0.0007$) fertilisation elicited decrease in Akt specific reversible thiol oxidation, as determined by ALISA wherein F-MAL is normalised to F–NHS, in 2-cell zygotes compared to unfertilised eggs. C. Confirmation of a significant ($P = <0.0001$) fertilisation induced decrease in Akt specific F-MAL fluorescence in zygotes compared to unfertilised eggs in new samples. D. A significant ($P = <0.0001$) fertilisation elicited decrease in Akt specific reversible thiol oxidation, as determined by ALISA-ELISA wherein F-MAL is normalised to total Akt using a biotin-conjugated detector antibody, in 2-cell zygotes compared to unfertilised eggs. In panels A–D, *P* values are derived from unpaired t-tests and unfertilised eggs and 2-cell zygotes ($n = 8$) datapoints are the product of 20 *X. laevis* unfertilised eggs/zygotes (i.e., 20 were homogenised to produce a single sample). E. Specificity of ALISA in unfertilised eggs and 2-cell zygotes compared to recombinant human Akt (i.e., positive control) and isotype IG (i.e., negative control). Statistical significance was determined using a one-way ANOVA with Tuckey post-hoc testing. F. No significant (unpaired *t*-test, $P = 0.5019$) random binding of F-MAL decorated proteins from a fully labelled standard added to isotype IG wells compared to Tris blocked blank control wells. G. A significant (paired-test, $P = 0.0015$) decrease in recombinant human Akt activity in equimolar NEM quenched ($n = 3$) compared to unquenched DTT ($n = 3$) wells.

our Akt finding was part of a homogenous or otherwise fertilisation induced change in protein thiol redox state within the kinase family. Microplate ALISA in F–NHS mode detected no fertilisation induced change in Src redox state (Fig. 5A). In the absence of a suitable biotin-conjugated detector antibody, we created macroscale immunoprecipitation (IP) ALISA. After verifying successful Src IP by immunoblot (Fig. 5B), we separated the Src and capture antibody F–NHS signals by non-reducing SDS-PAGE, excised the Src specific band, and passively eluted Src to measure its redox state in a microplate. IP ALISA confirms that Src specific reversible thiol oxidation is impervious to fertilisation: the redox state of Src remains the same before and after fertilisation (Fig. 5C). Micro and macroscale ALISA experiments reveal no impact of fertilisation (at the measured time-point) on Src specific reversible thiol oxidation. The impact of fertilisation on protein kinase redox state is, therefore, heterogenous. Provided a suitable capture antibody is available, Src supports the wider ability of ALISA to measure the redox state of the selected target.

3. Discussion

Measuring protein thiol redox state is central to understanding redox signalling in health and disease [18–21]. The lack of a microplate assay to measure protein thiol redox state rate-limits progress on accessibility grounds: redox proteomics is inaccessible to most. Widening access can accelerate discovery. Precedent exists. Plate reader compatible assays to measure ROS [7], antioxidant enzyme activity and/or content [8], and oxidised macromolecule adducts [3] advanced knowledge of oxidative stress by implicating ROS induced oxidative damage in disease. To meet the pressing need to measure target specific protein thiol redox state in a microplate we have developed ALISA. ALISA enables one to fulfil Halliwell and Whiteman's [10] first criteria for implicating ROS in disease adapted for redox signalling: the target specific redox signal induced by the experimental stimuli/state should be demonstratable (i.e., measurable). The ability to use ALISA to demonstrate the target protein specific redox signal in an accessible microplate format should accelerate current knowledge of protein thiol redox biology.

In the present work, we used ALISA to advance knowledge of developmental redox biology by unravelling the impact of fertilisation on the redox state of Akt. Akt is a strategically important redox regulated serine/threonine protein kinase responsive to several fundamental stimuli (e.g., insulin) in health and disease [40,41,52]. ALSA reveals that fertilisation decreased Akt specific reversible thiol oxidation. Interpretationally, decreased reversible thiol oxidation reflects a change in the rate of Akt specific reversible thiol oxidation formation and/or removal. Given the need to maintain the target in a native state for capture antibody binding, a change in protein structure (e.g., enabling F-MAL to label so-called cryptic thiols [53]) might also contribute. ALISA enabled us to meet a fundamental redox signalling criterion by demonstrating a fertilisation induced change in Atk specific redox state. A finding that is consistent with the central tenet of the redox theory of development: protein thiol mediated redox signalling regulates development [54]. Unravelling whether the redox state change is functional (i.e., a *bone fide* context specific redox signal) provides fertile ground for future work. Decreased reversible thiol oxidation could activate [40] or inhibit [41] Akt activity to regulate fertilisation induced PI3K signalling [49,55,56]. A change in Akt redox state might regulate the cell cycle. Based on serine 473 (S473) phosphorylation [57], Akt becomes active when cell cycle checkpoints come into force. Before then, a series of rapid checkpoint free cell cycles the zygote to go from 1 to 4000 cells in 6 h in *X. laevis* [58]. In this regard, ALISA could be used to assess the redox state of S437 phosphorylated compared to total Akt.

Beyond development, ALISA could be used to advance knowledge of protein thiol redox state in diverse fields (e.g., assisted reproduction, exercise, and neuroscience [59–62]). For example, one can now measure: circadian redox signalling via clock [63], exercise induced redox signalling via KEAP [64–66], sleep redox signalling via potassium channels [67], metabolic redox signalling via PKM2 [68], calcium redox signalling via STIM2 [69], mitochondrial redox signalling via ND3 [70–72], and many more in a microplate. ALISA is a valid technique to measure the redox state of such targets in a time- and cost-efficient manner. Time- and cost-efficiency is key. For example, one can now rapidly screen target thiol specific redox state to select proteins for targeted redox proteomics. The two techniques are highly complementary: ALISA measures global target redox state as the weighted mean of all modifiable thiols whereas targeted redox proteomics reports the individual redox state of all mass spectrometry detectable thiols. Combining the two techniques could capture otherwise undetectable redox changes: individual thiol changes that fail to shift the aggregated mean (see below) and redox proteomic undetectable reversible oxidised thiols. Measurement usually precedes manipulation. ALISA can rationalise the use of and validate (i.e., a change in target specific thiol redox state) chemical and genetic approaches to manipulate protein thiol redox state. In considering Akt, ALISA rationalises cysteine mutagenesis to unravel the functional impact of genetically disabling redox switches (e.g., Cys60 and 77) on fertilisation induced egg activation and the early cell cycle. Overall, ALISA is a valuable new tool to study target specific protein thiol redox state.

Despite many advantages, some drawbacks of ALISA should be considered. First, ALISA cannot compute protein thiol redox state in percentages. However, the feat has only recently been achieved in redox proteomics [43]. As numerous examples from the literature attest [3], quantifying a fold change is sufficient to discover new redox biology. Second, quantifying the total target specific thiol redox state, renders ALISA insensitive to changes in individual thiols that fail to shift the aggregated mean. This point may explain our Src finding. However, all current immunological techniques are insensitive to changes in individ-

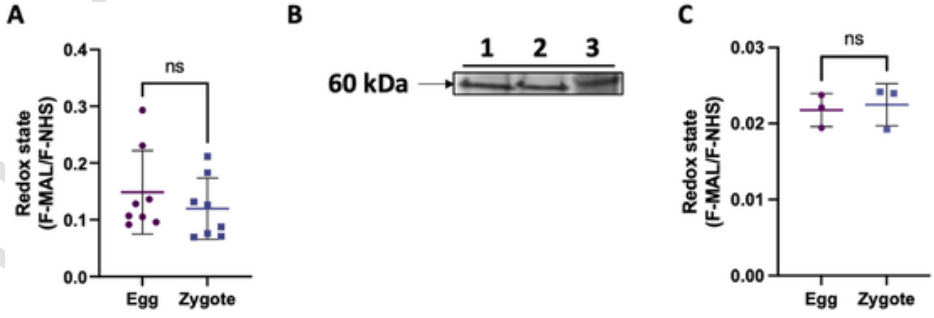

Fig. 5. No impact of fertilisation on Src specific thiol redox state. A. No significant (independent Student's t-test $P = 0.3857$) impact of fertilisation ($n = 8$) on Src specific thiol redox state as assessed by microscale ALISA (see main text) in *X. laevis*. B. Immunoprecipitation (IP) eluent Src immunoblot from unfertilised eggs (lane 1), zygotes (lane 2) and lysates (lane 3). C. No significant (independent Student's t-test $P = 0.7505$) impact of fertilisation ($n = 3$) on Src specific thiol redox state as assessed by IP-ALISA (see main text). Datapoints (i.e., each n value) are the product of 20 *X. laevis* unfertilised eggs/zygotes (i.e., 20 were homogenised to produce a single sample). The uncropped image for panel 5B is presented in supplementary Fig. 1.

ual thiols that fail to shift the aggregated mean [44]. Individual thiol changes can, however, be quantified using complementary targeted redox proteomic workflows [70,73]. Third, all immunological assays require a suitable antibody [44]. While an F–NHS reporter eliminates the need for matched pairs, one can only use ALISA in antibody compatible species. Compatibility concerns are limiting because of the foundational importance of yeast, worm, and fly work (e.g. [74–77]). Given their amenability to genome engineering, it may be possible to capture labelled (i.e., *N*-terminal FLAG decorated targets) target thiols to measure their redox state using a label specific antibody (i.e., anti-FLAG). Or alternatively use a specific small-molecule (i.e., inhibitor), substrate, or peptide aptamer to bind the target and thereby create antibody free ALISA.

4. Conclusion

To summarise, we have developed ALISA to measure target specific protein thiol redox state in a microplate. ALISA creates a widely accessible plate reader route to accelerate knowledge of protein thiol mediated redox signalling in health and disease. ALISA removes an accessibility impediment to studying protein thiol biology. Given plate reader compatible assays were instrumental in understanding oxidative stress, the consequences of widening access to redox signalling could be significant. Our proof-of-principle Akt studies show that ALISA can be used to demonstrate that an experimental stimulus or state induces a target specific redox signal. Measuring the change is the essential prelude to discovering new redox biology by chemically or genetically manipulating target thiol redox state.

5. Methods

5.1. Samples

Following ethical approval (#ETH2021-0222), adult *X. laevis* females were maintained at the European *Xenopus* Resource Centre (EXRC) at 18ºC. Unfertilised eggs and 2-cell zygotes collected 90 min post-fertilisation (hereafter samples) were harvested in batches of 20. Consistent with the ARRIVE guidelines [78], samples were derived from three different adult females and batched to minimise the possibility of results being attributable to any one female or outliers, respectively. Samples were lysed in ice-cold IP buffer (25 mM Tris-HCl pH 7.2, 150 mM NaCl, 1 mM EDTA, 1% NP-40 and 5% glycerol) supplemented with a protease inhibitor tablet (Sigma, UK, #11697498001) and 50 mM NEM (ThermoFisher, UK, #23030).

5.2. Thiol labelling

For the experiments presented in Figs. 4 and 5, samples were incubated with NEM for 30 min on ice to alkylate reduced thiols via a thioether bond before being centrifuged at 14,000 *g* for 5 min. Soluble supernatants were passed through a 6000 kDa cut-off spin column (Bio-Rad, UK, #7326222) to remove excess NEM. Samples were treated with 5 mM DTT for 30 min on ice to reduce reversibly oxidised thiols to the sulfhydryl state for F-MAL labelling. DTT was preferred to Tris(2-carboxyethyl)phosphine (TCEP) because the latter abrogates the F-MAL signal [79]. After removing excess DTT with a spin column, samples were incubated with 1 mM F-MAL (ThermoFisher, UK, #F150) to label reversibly oxidised thiols for 30 min on ice. To produce fully labelled standards (i.e., for experiments presented in Fig. 3), samples were reduced with 5 mM DTT at lysis before being treated with 1 mM F-MAL or 10 mM NEM for 30 min on ice. After removing excess F-MAL or NEM with a spin column, samples were mixed to produce the desired redox states described in Fig. 2. For example, to produce the 20% reversibly oxidised state 2 μl of completely F-MAL labelled standard was mixed with 8 μl of completely NEM labelled standard.

5.3. Covalently immobilising the capture antibody to an epoxy functionalised microplate

For experiments described in Figs. 2–5, epoxy group functionalised plates (PolyAn, Germany, #00695251) were treated with 100 ng *anti*-Akt1-3 (Abcam, UK, #ab179463), *anti*-Src (ThermoFisher, UK, #MA5-15214), or rabbit IG isotype control (ThermoFisher, UK, #31235) capture antibodies in binding buffer (Na_2HPO_4, 50 mM NaCl, pH 8.5) overnight at 4ºC with gentle agitation. Unreacted epoxy groups were blocked with (100 mM Tris, pH 9.0) for 90 min at room temperature (RT) with gentle agitation. Blocked plates were washed four times in PBST (0.05% Tween-20 in PBS, Sigma, UK, #P9416). For the experiments described in Fig. 2, IG isotype controls were labelled with 350 μM F–NHS for 30 min at RT (ThermoFisher, UK, AlexaFluor™647 conjugated NHS, #A37573) and the excess was removed with a spin column. The resultant F–NHS labelled IG control was incubated with the epoxy plate as described above and binding capacity was assessed by measuring the F–NHS signal in a plate reader after washing. To check covalent bonding, the IG-F-NHS treated wells were incubated with 2X bromophenol blue free non-reducing loading buffer (4% SDS, 100 mM Tris, 20% glycerol, pH 6.8) for 1 h at RT with vigorous shaking. IG F–NHS presence in the resulting eluents was assessed by measuring the F–NHS signal in a plate reader and by immunoblot using an anti-rabbit IG secondary antibody.

5.4. ALISA

For the experiments described in Figs. 4 and 5, samples (1–2 μg diluted 1:5 in PBS supplemented with a protease inhibitor tablet) were incubated with the capture antibody functionalised or IG control functionalised epoxy microplate for 2 h at RT in the dark with gentle agitation. Unbound samples were removed and capture antibody-target complexes were washed four times in PBST. Washed capture antibody-target complexes were treated with 350 μM F–NHS for 30 min at RT. Wells were washed (3 × 5 min) in PBST before a final PBS wash. Targets were eluted in loading buffer for 30 min on a plate shaker at 500 rpm. Successful elution was checked by measuring the F-MAL signal in the epoxy plate. Target specific F–NHS and F-MAL signals were measured for 100 ms at 494/518 and 651/671 nm in a new microplate using a plate reader. After subtracting background, target specific reversible thiol oxidation was calculated as: F-MAL/F–NHS.

5.5. ELISA-ALISA

For the experiments detailed in Fig. 4C–D, reagents from a commercial Akt ELISA (ThermoFisher, UK, #KHO0101) were used according to the assay guidelines with a few modifications. First, the capture Akt1-3 (Abcam, UK, #ab179463) antibody was bound to an epoxy functionalised microplate, as described above. Second, the HRP reaction was stopped in loading buffer to present all the target F-MAL groups for measurement (i.e., prevent steric masking due to the epitope-paratope binding) before adding the sulfuric acid stop solution to prevent it destroying the fluorophore. The 3,3′,5,5′-Tetramethylbenzidine colour change induced by the stop solution was measured at 450 nm on a plate reader for 100 ms.

5.6. IP-ALISA

Src capture antibody aliquots (5 μl) were incubated with 35 μl of protein G derivatised magnetic beads (ThermoFisher, UK, # 10003D) for 1 h at RT with gentle agitation. Beads were magnetised to remove unbound capture antibody. Samples (~500 μg, diluted 1:1 in PBS supplemented with a protease inhibitor tablet) were incubated with the capture antibody functionalised beads overnight with gentle agitation at 4ºC. Excess samples were removed, beads were washed twice in

PBST, and incubated with 350 μM F–NHS for 30 min at RT. Excess F–NHS was removed by magnetising the beads, transferring them to a new Eppendorf, and additional washing (2 x PBST). Capture antibody-target complexes were eluted by boiling in loading buffer for 5 min at 80ºC. Samples were resolved by non-reducing SDS-PAGE to hold the capture antibody at ~150 kDa by keeping the intrachain disulfide bonds intact (verified by immunoblot, data available on request), before the Src specific band was manually excised and passively eluted in distilled H_2O for 24 h at RT. Src specific reversible thiol oxidation was measured on a plate reader as above. To check IP success, eluent Src immunoblots were performed.

5.7. Click-PEG

For the experiment described in supplementary Figure 1, samples were prepared for Click-PEG as above except we substituted F-MAL for 5 mM dibenzocyclooctyne PEG4 maleimide [45,46]. After determining protein content with a BCA assay, 20 μg protein aliquots were incubated with 1 mM azide functionalised PEG-5000 kDa (Sigma, UK, #81323, respectively) to initiate the catalyst-free strained-promoted azide alkyne cycloaddition (SPAAC) reaction [80] overnight at RT with gentle agitation in loading buffer. Negative controls (i.e., NEM labelled samples) were treated identically.

5.8. Immunoblotting

Samples were resolved by SDS-PAGE on precast 4–15% gradient gels (BioRad, UK, #4561085). Gels were transferred onto a 0.45 μM low auto-fluorescence PVDF membrane (ThermoFisher, UK, #LC2005) and blocked for 2 h at RT in 5% non-fat-dry milk (NFDM) in Tris buffered saline supplemented with 1% Tween-20 (TBST) [81]. Membranes were incubated with rabbit primary Akt1-3 antibody (1:1000 in TBST with 3% NFDM) overnight at 4ºC, washed in TBST, incubated with alkaline phosphatase conjugated rabbit or mouse (Abcam, UK, # ab6722 & ab97020) secondary antibody for 1 h at RT, washed in TBST, and incubated with substrate (Sigma, UK, #B5655) until colour development occurred. Blots were imaged on an Analytic Jena gel scanner.

5.9. Akt activity assay

Akt activity was measured on a plate reader using a commercial kit (Abcam, UK, # ab139436) according to the manufacturer's protocol. To study redox state, an equimolar (2 mM) amount of NEM was added to the DTT containing kinase assay buffer for 15 min before adding recombinant Akt and ATP to initiate the assay. No activity was observed when the kinase assay buffer was passed through a spin column likely due to the presence of essential low molecular weight constituents (data available on request).

5.10. Statistics

Data set normality was assessed using D'Agostino-Pearson and Shapiro-Wilk testing with alpha ≥0.05. Based on their normality, data sets were analysed using the relevant parametric or non-parametric test with post-hoc testing as appropriate on Graph Pad prism version 9 with alpha ≤0.05. Figure legends report the statistical test (s) used. Data are presented as Mean (M) and standard deviation (SD).

Funding

J.N.C. received Tenovus (#G19.03), and Rosetrees Trust (#A2819), and Carnegie Trust (#RIG009262) funding. A.N. and M.G. are funded by the Wellcome Trust (212942/Z/18/Z) and BBSRC (BB/R014841/1).

Acknowledgments

The authors thank the funders who made the present work possible. The graphical abstract and Fig. 1 were created using Biorender (www.Biorender.com). The manuscript is dedicated to the memory of Mary "Isabel" Marteau (1923-2019).

Appendix A. Supplementary data

Supplementary data to this article can be found online at https://doi.org/10.1016/j.freeradbiomed.2021.08.018.

Akt cysteines

Akt	*Xenopus*	Human	Oximouse	Annotated
1	6: Cys: 60,77, 225, 297, 311, 345, (Q98TY9)	7: 60, 77, 224, 297, 310, 344, 460 (P31749)	4 residues: 60, 77, 296, 311	60-77 is an activating RSSR 297-311 is an inhibitory RSSR
2	6: Cys: 62, 79, 231, 302, 316, 350 (Q7ZX15)*	7: 60, 77, 124, 226, 297, 311, 345 (P31751)	4 residues: 60, 124, 297, 311	60-77 is an activating RSSR 297-311 is an inhibitory RSSR
3	No entry in Xenbase.	8: 59, 76, 119, 222, 293, 307, 341, 459, (Q9Y243)	No data.	n/a

* No difference between L and S.

Links: https://oximouse.hms.harvard.edu/sites.html
http://www.xenbase.org/gene/searchGene.do?method=search&searchIn=0&searchValue=akt3+xenopus&searchType=0.

References

[1] C.C. Winterbourn, Reconciling the chemistry and biology of reactive oxygen species, Nat. Chem. Biol. 4 (2008) 278–286, https://doi.org/10.1038/nchembio.85.
[2] B.C. Dickinson, C.J. Chang, Chemistry and biology of reactive oxygen species in signaling or stress responses, Nat. Chem. Biol. 7 (2011) 504–511, https://doi.org/10.1038/nchembio.607.
[3] B. H, J. Gutteridge, Free Radicals in Biology and Medicine, 2015.
[4] M.P. Murphy, A. Holmgren, N.-G. Larsson, B. Halliwell, C.J. Chang, B. Kalyanaraman, S.G. Rhee, P.J. Thornalley, L. Partridge, D. Gems, T. Nyström, V. Belousov, P.T. Schumacker, C.C. Winterbourn, Unraveling the biological roles of reactive oxygen species, Cell Metabol. 13 (2011) 361–366, https://doi.org/10.1016/j.cmet.2011.03.010.
[5] M. Schwarzländer, T.P. Dick, A.J. Meyer, B. Morgan, Dissecting redox biology using fluorescent protein sensors, Antioxidants Redox Signal. 24 (2016) 680–712, https://doi.org/10.1089/ars.2015.6266.
[6] H.J. Forman, O. Augusto, R. Brigelius-Flohe, P.A. Dennery, B. Kalyanaraman, H. Ischiropoulos, G.E. Mann, R. Radi, L.J. Roberts, J. Vina, K.J.A. Davies, Even free radicals should follow some rules: a Guide to free radical research terminology and methodology, Free Radical Bio Med 78 (2015) 233–235, https://doi.org/10.1016/j.freeradbiomed.2014.10.504.
[7] J. Zielonka, B. Kalyanaraman, Small-molecule luminescent probes for the detection

of cellular oxidizing and nitrating species, Free Radical Bio Med 128 (2018) 3–22, https://doi.org/10.1016/j.freeradbiomed.2018.03.032.
[8] N.V. Margaritelis, J.N. Cobley, V. Paschalis, A.S. Veskoukis, A.A. Theodorou, A. Kyparos, M.G. Nikolaidis, Going retro: oxidative stress biomarkers in modern redox biology, Free Radical Bio Med 98 (2016) 2–12, https://doi.org/10.1016/j.freeradbiomed.2016.02.005.
[9] J.N. Cobley, G.K. Sakellariou, D.J. Owens, S. Murray, S. Waldron, W. Gregson, W.D. Fraser, J.G. Burniston, L.A. Iwanejko, A. McArdle, J.P. Morton, M.J. Jackson, G.L. Close, Lifelong training preserves some redox-regulated adaptive responses after an acute exercise stimulus in aged human skeletal muscle, Free Radical Bio Med 70 (2014) 23–32, https://doi.org/10.1016/j.freeradbiomed.2014.02.004.
[10] B. Halliwell, M. Whiteman, Measuring reactive species and oxidative damage in vivo and in cell culture: how should you do it and what do the results mean?, Brit J Pharmacol 142 (2004) 231–255, https://doi.org/10.1038/sj.bjp.0705776.
[11] H.J. Forman, H. Zhang, Targeting oxidative stress in disease: promise and limitations of antioxidant therapy, Nat. Rev. Drug Discov. (2021) 1–21, https://doi.org/10.1038/s41573-021-00233-1.
[12] H. Sies, Oxidative eustress: on constant alert for redox homeostasis, Redox Biol 41 (2021) 101867, https://doi.org/10.1016/j.redox.2021.101867.
[13] H. Sies, C. Berndt, D.P. Jones, Oxidative stress, Annu. Rev. Biochem. 86 (2016) 1–34, https://doi.org/10.1146/annurev-biochem-061516-045037.
[14] H. Sies, Oxidative stress: a concept in redox biology and medicine, Redox Biol 4 (2015) 180–183, https://doi.org/10.1016/j.redox.2015.01.002.
[15] D.P. Jones, Redefining oxidative stress, Antioxidants Redox Signal. 8 (2006) 1865–1879, https://doi.org/10.1089/ars.2006.8.1865.
[16] H. Sies, Oxidative Stress, Academic Press, 2019.
[17] S. Parvez, M.J.C. Long, J.R. Poganik, Y. Aye, Redox signaling by reactive electrophiles and oxidants, Chem. Rev. 118 (2018) 8798–8888, https://doi.org/10.1021/acs.chemrev.7b00698.
[18] C.E. Paulsen, K.S. Carroll, Cysteine-mediated redox signaling: chemistry, biology, and tools for discovery, Chem. Rev. 113 (2013) 4633–4679, https://doi.org/10.1021/cr300163e.
[19] K.M. Holmström, T. Finkel, Cellular mechanisms and physiological consequences of redox-dependent signalling, Nat. Rev. Mol. Cell Biol. 15 (2014) 411–421, https://doi.org/10.1038/nrm3801.
[20] H. Sies, D.P. Jones, Reactive oxygen species (ROS) as pleiotropic physiological signalling agents, Nat. Rev. Mol. Cell Biol. 21 (2020) 363–383, https://doi.org/10.1038/s41580-020-0230-3.
[21] C.C. Winterbourn, M.B. Hampton, Thiol chemistry and specificity in redox signaling, Free Radical Bio Med 45 (2008) 549–561, https://doi.org/10.1016/j.freeradbiomed.2008.05.004.
[22] M.C. Sobotta, W. Liou, S. Stöcker, D. Talwar, M. Oehler, T. Ruppert, A.N.D. Scharf, T.P. Dick, Peroxiredoxin-2 and STAT3 form a redox relay for H2O2 signaling, Nat. Chem. Biol. 11 (2015) 64–70, https://doi.org/10.1038/nchembio.1695.
[23] D. Talwar, J. Messens, T.P. Dick, A role for annexin A2 in scaffolding the peroxiredoxin 2–STAT3 redox relay complex, Nat. Commun. 11 (2020) 4512, https://doi.org/10.1038/s41467-020-18324-9.
[24] S. Stöcker, M. Maurer, T. Ruppert, T.P. Dick, A role for 2-Cys peroxiredoxins in facilitating cytosolic protein thiol oxidation, Nat. Chem. Biol. 14 (2018) 148–155, https://doi.org/10.1038/nchembio.2536.
[25] D. Young, B. Pedre, D. Ezeriņa, B.D. Smet, A. Lewandowska, M.-A. Tossounian, N. Bodra, J. Huang, L.A. Rosado, F.V. Breusegem, J. Messens, Protein promiscuity in H2O2 signaling, Antioxidants Redox Signal. 30 (2018) 1285–1324, https://doi.org/10.1089/ars.2017.7013.
[26] J.M. Held, Redox systems biology: harnessing the sentinels of the cysteine redoxome, Antioxidants Redox Signal. 32 (2020) 659–676, https://doi.org/10.1089/ars.2019.7725.
[27] Y.-M. Go, J.D. Chandler, D.P. Jones, The cysteine proteome, Free Radical Bio Med 84 (2015) 227–245, https://doi.org/10.1016/j.freeradbiomed.2015.03.022.
[28] D.P. Jones, H. Sies, The redox code, Antioxidants Redox Signal. 23 (2015) 734–746, https://doi.org/10.1089/ars.2015.6247.
[29] X. Huang, S. Chen, W. Li, L. Tang, Y. Zhang, N. Yang, Y. Zou, X. Zhai, N. Xiao, W. Liu, P. Li, C. Xu, ROS regulated reversible protein phase separation synchronizes plant flowering, Nat. Chem. Biol. 17 (2021) 549–557, https://doi.org/10.1038/s41589-021-00739-0.
[30] H. Kim, S. Ha, H.Y. Lee, K. Lee, ROSics: chemistry and proteomics of cysteine modifications in redox biology, Mass Spectrom. Rev. 34 (2015) 184–208, https://doi.org/10.1002/mas.21430.
[31] J. Yang, K.S. Carroll, D.C. Liebler, The expanding landscape of the thiol redox proteome*, Mol. Cell. Proteomics 15 (2016) 1–11, https://doi.org/10.1074/mcp.o115.056051.
[32] J.N. Cobley, G.K. Sakellariou, H. Husi, B. McDonagh, Proteomic strategies to unravel age-related redox signalling defects in skeletal muscle, Free Radical Bio Med 132 (2019) 24–32, https://doi.org/10.1016/j.freeradbiomed.2018.09.012.
[33] Y. Shi, K.S. Carroll, Parallel evaluation of nucleophilic and electrophilic chemical probes for sulfenic acid: reactivity, selectivity and biocompatibility, Redox Biol 46 (2021) 102072, https://doi.org/10.1016/j.redox.2021.102072.
[34] H.M. Cochemé, C. Quin, S.J. McQuaker, F. Cabreiro, A. Logan, T.A. Prime, I. Abakumova, J.V. Patel, I.M. Fearnley, A.M. James, C.M. Porteous, R.A.J. Smith, S. Saeed, J.E. Carré, M. Singer, D. Gems, R.C. Hartley, L. Partridge, M.P. Murphy, Measurement of H2O2 within living Drosophila during aging using a ratiometric mass spectrometry probe targeted to the mitochondrial matrix, Cell Metabol. 13 (2011) 340–350, https://doi.org/10.1016/j.cmet.2011.02.003.
[35] V.V. Pak, D. Ezeriņa, O.G. Lyublinskaya, B. Pedre, P.A. Tyurin-Kuzmin, N.M. Mishina, M. Thauvin, D. Young, K. Wahni, S.A.M. Gache, A.D. Demidovich, Y.G. Ermakova, Y.D. Maslova, A.G. Shokhina, E. Eroglu, D.S. Bilan, I. Bogeski, T. Michel, S. Vriz, J. Messens, V.V. Belousov, Ultrasensitive genetically encoded indicator for hydrogen peroxide identifies roles for the oxidant in cell migration and mitochondrial function, Cell Metabol. 31 (2020) 642–653, e6, https://doi.org/10.1016/j.cmet.2020.02.003.
[36] M.M. Shchepinova, A.G. Cairns, T.A. Prime, A. Logan, A.M. James, A.R. Hall, S. Vidoni, S. Arndt, S.T. Caldwell, H.A. Prag, V.R. Pell, T. Krieg, J.F. Mulvey, P. Yadav, J.N. Cobley, T.P. Bright, H.M. Senn, R.F. Anderson, M.P. Murphy, R.C. Hartley, MitoNeoD: a mitochondria-targeted superoxide probe, Cell Chem Biol 24 (2017) 1285–1298, e12, https://doi.org/10.1016/j.chembiol.2017.08.003.
[37] R.E. Hansen, J.R. Winther, An introduction to methods for analyzing thiols and disulfides: reactions, reagents, and practical considerations, Anal. Biochem. 394 (2009) 147–158, https://doi.org/10.1016/j.ab.2009.07.051.
[38] Y. Shi, K.S. Carroll, Activity-based sensing for site-specific proteomic analysis of cysteine oxidation, Accounts Chem. Res. 53 (2020) 20–31, https://doi.org/10.1021/acs.accounts.9b00562.
[39] L.J. Alcock, M.V. Perkins, J.M. Chalker, Chemical methods for mapping cysteine oxidation, Chem. Soc. Rev. 47 (2017) 231–268, https://doi.org/10.1039/c7cs00607a.
[40] Z. Su, J.G. Burchfield, P. Yang, S.J. Humphrey, G. Yang, D. Francis, S. Yasmin, S.-Y. Shin, D.M. Norris, A.L. Kearney, M.A. Astore, J. Scavuzzo, K.H. Fisher-Wellman, Q.-P. Wang, B.L. Parker, G.G. Neely, F. Vafaee, J. Chiu, R. Yeo, P.J. Hogg, D.J. Fazakerley, L.K. Nguyen, S. Kuyucak, D.E. James, Global redox proteome and phosphoproteome analysis reveals redox switch in Akt, Nat. Commun. 10 (2019) 5486, https://doi.org/10.1038/s41467-019-13114-4.
[41] R. Wani, J. Qian, L. Yin, E. Bechtold, S.B. King, L.B. Poole, E. Paek, A.W. Tsang, C.M. Furdui, Isoform-specific regulation of Akt by PDGF-induced reactive oxygen species, Proc. Natl. Acad. Sci. Unit. States Am. 108 (2011) 10550–10555, https://doi.org/10.1073/pnas.1011665108.
[42] E. Sidlauskaite, J.W. Gibson, I.L. Megson, P.D. Whitfield, A. Tovmasyan, I. Batinic-Haberle, M.P. Murphy, P.R. Moult, J.N. Cobley, Mitochondrial ROS cause motor deficits induced by synaptic inactivity: implications for synapse pruning, Redox Biol 16 (2018) 344–351, https://doi.org/10.1016/j.redox.2018.03.012.
[43] H. Xiao, M.P. Jedrychowski, D.K. Schweppe, E.L. Huttlin, Q. Yu, D.E. Heppner, J. Li, J. Long, E.L. Mills, J. Szpyt, Z. He, G. Du, R. Garrity, A. Reddy, L.P. Vaites, J.A. Paulo, T. Zhang, N.S. Gray, S.P. Gygi, E.T. Chouchani, A quantitative tissue-specific landscape of protein redox regulation during aging, Cell 180 (2020) 968–983, e24, https://doi.org/10.1016/j.cell.2020.02.012.
[44] J.N. Cobley, H. Husi, Immunological techniques to assess protein thiol redox state: opportunities, challenges and solutions, Antioxidants 9 (2020) 315, https://doi.org/10.3390/antiox9040315.
[45] L.A.G. van Leeuwen, E.C. Hinchy, M.P. Murphy, E.L. Robb, H.M. Cochemé, Click-PEGylation – a mobility shift approach to assess the redox state of cysteines in candidate proteins, Free Radical Bio Med 108 (2017) 374–382, https://doi.org/10.1016/j.freeradbiomed.2017.03.037.
[46] J.N. Cobley, A. Noble, E. Jimenez-Fernandez, M.-T.V. Moya, M. Guille, H. Husi, Catalyst-free Click PEGylation reveals substantial mitochondrial ATP synthase subunit alpha oxidation before and after fertilisation, Redox Biol 26 (2019) 101258, https://doi.org/10.1016/j.redox.2019.101258.
[47] J. Cobley, A. Noble, R. Bessell, M. Guille, H. Husi, Reversible thiol oxidation inhibits the mitochondrial ATP synthase in Xenopus laevis oocytes, Antioxidants 9 (2020) 215, https://doi.org/10.3390/antiox9030215.
[48] J.R. Burgoyne, O. Oviosu, P. Eaton, The PEG-switch assay: a fast semi-quantitative method to determine protein reversible cysteine oxidation, J. Pharmacol. Toxicol. 68 (2013) 297–301, https://doi.org/10.1016/j.vascn.2013.07.001.
[49] G. Mammadova, T. Iwasaki, A.A. Tokmakov, Y. Fukami, K. Sato, Evidence that phosphatidylinositol 3-kinase is involved in sperm-induced tyrosine kinase signaling in Xenopus egg fertilization, BMC Dev. Biol. 9 (2009) 68, https://doi.org/10.1186/1471-213x-9-68.
[50] D.E. Heppner, C.M. Dustin, C. Liao, M. Hristova, C. Veith, A.C. Little, B.A. Ahlers, S. L. White, B. Deng, Y.-W. Lam, J. Li, A. van der Vliet, Direct cysteine sulfenylation drives activation of the Src kinase, Nat. Commun. 9 (2018) 4522, https://doi.org/10.1038/s41467-018-06790-1.
[51] K. Sato, M. Aoto, K. Mori, S. Akasofu, A.A. Tokmakov, S. Sahara, Y. Fukami, Purification and characterization of a src-related p57 protein-tyrosine kinase from Xenopus oocytes isolation OF an inactive form OF the enzyme and its activation and translocation UPON fertilization*, J. Biol. Chem. 271 (1996) 13250–13257, https://doi.org/10.1074/jbc.271.22.13250.
[52] C. Lennicke, H.M. Cochemé, Redox regulation of the insulin signalling pathway, Redox Biol 42 (2021) 101964, https://doi.org/10.1016/j.redox.2021.101964.
[53] J.B. Behring, S. van der Post, A.D. Mooradian, M.J. Egan, M.I. Zimmerman, J.L. Clements, G.R. Bowman, J.M. Held, Spatial and temporal alterations in protein structure by EGF regulate cryptic cysteine oxidation, Sci. Signal. 13 (2020) eaay7315, https://doi.org/10.1126/scisignal.aay7315.
[54] J.M. Hansen, D.P. Jones, C. Harris, The redox theory of development, Antioxidants Redox Signal. 32 (2020) 715–740, https://doi.org/10.1089/ars.2019.7976.
[55] N. Nader, R.P. Kulkarni, M. Dib, K. Machaca, How to make a good egg! the need for remodeling of oocyte Ca2+ signaling to mediate the egg-to-embryo transition, Cell Calcium 53 (2013) 41–54, https://doi.org/10.1016/j.ceca.2012.11.015.
[56] D. Clift, M. Schuh, Restarting life: fertilization and the transition from meiosis to mitosis, Nat. Rev. Mol. Cell Biol. 14 (2013) 549–562, https://doi.org/10.1038/nrm3643.
[57] C.V. Finkielstein, A.L. Lewellyn, J.L. Maller, The midblastula transition in Xenopus embryos activates multiple pathways to prevent apoptosis in response to DNA damage, Proc. Natl. Acad. Sci. Unit. States Am. 98 (2001) 1006–1011, https://doi.org/10.1073/pnas.98.3.1006.
[58] E. Hörmanseder, T. Tischer, T.U. Mayer, Modulation of cell cycle control during

oocyte-to-embryo transitions, EMBO J. 32 (2013) 2191–2203, https://doi.org/10.1038/emboj.2013.164.
[59] J.N. Cobley, Mechanisms of mitochondrial ROS production in assisted reproduction: the known, the unknown, and the intriguing, Antioxidants 9 (2020) 933, https://doi.org/10.3390/antiox9100933.
[60] J.N. Cobley, M.L. Fiorello, D.M. Bailey, 13 reasons why the brain is susceptible to oxidative stress, Redox Biol 15 (2018) 490–503, https://doi.org/10.1016/j.redox.2018.01.008.
[61] J.N. Cobley, Oxidative Stress, 2020, pp. 447–462, https://doi.org/10.1016/b978-0-12-818606-0.00023-7.
[62] J.N. Cobley, Synapse pruning: mitochondrial ROS with their hands on the shears, Bioessays 40 (2018) 1800031, https://doi.org/10.1002/bies.201800031.
[63] J.-F. Pei, X.-K. Li, W.-Q. Li, Q. Gao, Y. Zhang, X.-M. Wang, J.-Q. Fu, S.-S. Cui, J.-H. Qu, X. Zhao, D.-L. Hao, D. Ju, N. Liu, K.S. Carroll, J. Yang, E.E. Zhang, J.-M. Cao, H.-Z. Chen, D.-P. Liu, Diurnal oscillations of endogenous H2O2 sustained by p66Shc regulate circadian clocks, Nat. Cell Biol. 21 (2019) 1553–1564, https://doi.org/10.1038/s41556-019-0420-4.
[64] J.N. Cobley, G.L. Close, D.M. Bailey, G.W. Davison, Exercise redox biochemistry: conceptual, methodological and technical recommendations, Redox Biol 12 (2017) 540–548, https://doi.org/10.1016/j.redox.2017.03.022.
[65] J.N. Cobley, H. McHardy, J.P. Morton, M.G. Nikolaidis, G.L. Close, Influence of vitamin C and vitamin E on redox signaling: implications for exercise adaptations, Free Radical Bio Med 84 (2015) 65–76, https://doi.org/10.1016/j.freeradbiomed.2015.03.018.
[66] N.V. Margaritelis, J.N. Cobley, V. Paschalis, A.S. Veskoukis, A.A. Theodorou, A. Kyparos, M.G. Nikolaidis, Principles for integrating reactive species into in vivo biological processes: examples from exercise physiology, Cell. Signal. 28 (2016) 256–271, https://doi.org/10.1016/j.cellsig.2015.12.011.
[67] A. Kempf, S.M. Song, C.B. Talbot, G. Miesenböck, A potassium channel β-subunit couples mitochondrial electron transport to sleep, Nature 568 (2019) 230–234, https://doi.org/10.1038/s41586-019-1034-5.
[68] D. Anastasiou, G. Poulogiannis, J.M. Asara, M.B. Boxer, J. Jiang, M. Shen, G. Bellinger, A.T. Sasaki, J.W. Locasale, D.S. Auld, C.J. Thomas, M.G.V. Heiden, L.C. Cantley, Inhibition of pyruvate kinase M2 by reactive oxygen species contributes to cellular antioxidant responses, Science 334 (2011) 1278–1283, https://doi.org/10.1126/science.1211485.
[69] C.S. Gibhardt, S. Cappello, R. Bhardwaj, R. Schober, S.A. Kirsch, Z.B. del Rio, S. Gahbauer, A. Bochicchio, M. Sumanska, C. Ickes, I. Stejerean-Todoran, M. Mitkovski, D. Alansary, X. Zhang, A. Revazian, M. Fahrner, V. Lunz, I. Frischauf, T. Luo, D. Ezerina, J. Messens, V.V. Belousov, M. Hoth, R.A. Böckmann, M.A. Hediger, R. Schindl, I. Bogeski, Oxidative stress-induced STIM2 cysteine modifications suppress store-operated calcium entry, Cell Rep. 33 (2020) 108292, https://doi.org/10.1016/j.celrep.2020.108292.
[70] E.T. Chouchani, C. Methner, S.M. Nadtochiy, A. Logan, V.R. Pell, S. Ding, A.M. James, H.M. Cochemé, J. Reinhold, K.S. Lilley, L. Partridge, I.M. Fearnley, A.J. Robinson, R.C. Hartley, R.A.J. Smith, T. Krieg, P.S. Brookes, M.P. Murphy, Cardioprotection by S-nitrosation of a cysteine switch on mitochondrial complex I, Nat. Med. 19 (2013) 753–759, https://doi.org/10.1038/nm.3212.
[71] E.T. Chouchani, V.R. Pell, E. Gaude, D. Aksentijević, S.Y. Sundier, E.L. Robb, A. Logan, S.M. Nadtochiy, E.N.J. Ord, A.C. Smith, F. Eyassu, R. Shirley, C.-H. Hu, A.J. Dare, A.M. James, S. Rogatti, R.C. Hartley, S. Eaton, A.S.H. Costa, P.S. Brookes, S.M. Davidson, M.R. Duchen, K. Saeb-Parsy, M.J. Shattock, A.J. Robinson, L.M. Work, C. Frezza, T. Krieg, M.P. Murphy, Ischaemic accumulation of succinate controls reperfusion injury through mitochondrial ROS, Nature 515 (2014) 431–435, https://doi.org/10.1038/nature13909.
[72] P. Hernansanz-Agustín, C. Choya-Foces, S. Carregal-Romero, E. Ramos, T. Oliva, T. Villa-Piña, L. Moreno, A. Izquierdo-Álvarez, J.D. Cabrera-García, A. Cortés, A.V. Lechuga-Vieco, P. Jadiya, E. Navarro, E. Parada, A. Palomino-Antolín, D. Tello, R. Acín-Pérez, J.C. Rodríguez-Aguilera, P. Navas, Á. Cogolludo, I. López-Montero, Á. Martínez-del-Pozo, J. Egea, M.G. López, J.W. Elrod, J. Ruíz-Cabello, A. Bogdanova, J.A. Enríquez, A. Martínez-Ruiz, Na+ controls hypoxic signalling by the mitochondrial respiratory chain, Nature 586 (2020) 287–291, https://doi.org/10.1038/s41586-020-2551-y.
[73] J.M. Held, S.R. Danielson, J.B. Behring, C. Atsriku, D.J. Britton, R.L. Puckett, B. Schilling, J. Campisi, C.C. Benz, B.W. Gibson, Targeted quantitation of site-specific cysteine oxidation in endogenous proteins using a differential alkylation and multiple reaction monitoring mass spectrometry approach, Mol. Cell. Proteomics 9 (2010) 1400–1410, https://doi.org/10.1074/mcp.m900643-mcp200.
[74] J. Meng, L. Fu, K. Liu, C. Tian, Z. Wu, Y. Jung, R.B. Ferreira, K.S. Carroll, T.K. Blackwell, J. Yang, Global profiling of distinct cysteine redox forms reveals wide-ranging redox regulation in C. elegans, Nat. Commun. 12 (2021) 1415, https://doi.org/10.1038/s41467-021-21686-3.
[75] D. Knoefler, M. Thamsen, M. Koniczek, N.J. Niemuth, A.-K. Diederich, U. Jakob, Quantitative in vivo redox sensors uncover oxidative stress as an early event in life, Mol Cell 47 (2012) 767–776, https://doi.org/10.1016/j.molcel.2012.06.016.
[76] P.S. Amponsah, G. Yahya, J. Zimmermann, M. Mai, S. Mergel, T. Mühlhaus, Z. Storchova, B. Morgan, Peroxiredoxins couple metabolism and cell division in an ultradian cycle, Nat. Chem. Biol. 17 (2021) 477–484, https://doi.org/10.1038/s41589-020-00728-9.
[77] A. Vaccaro, Y.K. Dor, K. Nambara, E.A. Pollina, C. Lin, M.E. Greenberg, D. Rogulja, Sleep loss can cause death through accumulation of reactive oxygen species in the gut, Cell 181 (2020) 1307–1328, e15, https://doi.org/10.1016/j.cell.2020.04.049.
[78] N.P. du Sert, V. Hurst, A. Ahluwalia, S. Alam, M.T. Avey, M. Baker, W.J. Browne, A. Clark, I.C. Cuthill, U. Dirnagl, M. Emerson, P. Garner, S.T. Holgate, D.W. Howells, N. A. Karp, S.E. Lazic, K. Lidster, C.J. MacCallum, M. Macleod, E.J. Pearl, O.H. Petersen, F. Rawle, P. Reynolds, K. Rooney, E.S. Sena, S.D. Silberberg, T. Steckler, H. Würbel, The ARRIVE guidelines 2.0: updated guidelines for reporting animal research, PLoS Biol. 18 (2020) e3000410, https://doi.org/10.1371/journal.pbio.3000410.
[79] K. Tyagarajan, E. Pretzer, J.E. Wiktorowicz, Thiol-reactive dyes for fluorescence labeling of proteomic samples, Electrophoresis 24 (2003) 2348–2358, https://doi.org/10.1002/elps.200305478.
[80] N.J. Agard, J.A. Prescher, C.R. Bertozzi, A strain-promoted [3 + 2] Azide−Alkyne cycloaddition for covalent modification of biomolecules in living systems, J. Am. Chem. Soc. 126 (2004) 15046–15047, https://doi.org/10.1021/ja044996f.
[81] J.N. Cobley, G.K. Sakellariou, S. Murray, S. Waldron, W. Gregson, J.G. Burniston, J. P. Morton, L.A. Iwanejko, G.L. Close, Lifelong endurance training attenuates age-related genotoxic stress in human skeletal muscle, Longev. Heal. 2 (2013) 11, https://doi.org/10.1186/2046-2395-2-11.